SANDIA REPORT
SAND2001-0171
Unlimited Release
Printed January 2001

Dynamical Properties of Polymers: Computational Modeling

John G. Curro, Dana Rottach, and John D. McCoy

Prepared by
Sandia National Laboratories
Albuquerque, New Mexico 87185 and Livermore, California 94550

Sandia is a multiprogram laboratory operated by Sandia Corporation, a Lockheed Martin Company, for the United States Department of Energy under Contract DE-AC04-94AL85000.

Issued by Sandia National Laboratories, operated for the United States Department of Energy by Sandia Corporation.

Available to DOE and DOE contractors from
U.S. Department of Energy
Office of Scientific and Technical Information
P.O. Box 62
Oak Ridge, TN 37831

Telephone: (865)576-8401
Facsimile: (865)576-5728
E-Mail: reports@adonis.osti.gov
Online ordering: http://www.doe.gov/bridge

Available to the public from
U.S. Department of Commerce
National Technical Information Service
5285 Port Royal Rd
Springfield, VA 22161

Telephone: (800)553-6847
Facsimile: (703)605-6900
E-Mail: orders@ntis.fedworld.gov
Online order: http://www.ntis.gov/ordering.htm

SAND 2001-0171
Unlimited Release
Printed January 2001

Dynamical Properties of Polymers: Computational Modeling

LDRD Project: 10404

Final Report

John G. Curro
Sandia National Laboratories
P. O. Box 5800
Albuquerque, NM 87185-1349

Dana Rottach
University of New Mexico
Albuquerque, NM

John D. McCoy
New Mexico Institute of Mining & Technology
Socorro, NM

Abstract

The free volume distribution has been a qualitatively useful concept by which dynamical properties of polymers, such as the penetrant diffusion constant, viscosity, and glass transition temperature, could be correlated with static properties. In an effort to put this on a more quantitative footing, we define the free volume distribution as the probability of finding a spherical cavity of radius R in a polymer liquid. This is identical to the insertion probability in scaled particle theory, and is related to the chemical potential of hard spheres of radius R in a polymer in the Henry's law limit. We used the Polymer Reference Interaction Site Model (PRISM) theory to compute the free volume distribution of semiflexible polymer melts as a function of chain stiffness. Good agreement was found with the corresponding free volume distributions obtained from MD simulations. Surprisingly, the free volume distribution was insensitive to the chain stiffness, even though the single chain structure and the intermolecular pair correlation functions showed a strong dependence on chain stiffness. We also calculated the free volume distributions of polyisobutylene (PIB) and polyethylene (PE) at 298K and at elevated temperatures from PRISM theory. We found that PIB has more of its free volume distributed in smaller size cavities than for PE at the same temperature.

INTRODUCTION

The concept of free volume has a time honored tradition in polymer science and has been very useful in qualitatively explaining many phenomena associated with the local mobility of chains including: viscoelasticity[1], glass transition[2], physical aging[3,4], viscosity[5], and diffusion[6,7]. While being a qualitatively useful concept, very little work has been done to quantitatively apply free volume ideas to predict dynamical quantities. Free volume plays a central role in some equations of state. In fact, the free volume distribution enters directly into the scaled particle theory of Reiss and collaborators[8] for the equation of state of hard sphere liquids. For polymers, Simha and Somcynsky[9] introduced free volume into their equation of state of polymer melts and blends. Because of the lattice nature of the theory, the free volume in Simha - Somcynsky theory is quantized to large volumes of order of the monomer size. In the present investigation, we calculate the free volume distribution of polymer melts in continuous space.

The free volume distribution can be measured experimentally in various polymers with positron annihilation lifetime spectroscopy[10,11] (PALS). Correlations have been made between free volume distributions obtained from PALS and the equation-of-state[11], glass transition[11], physical aging[10], and gas diffusivity[12]. Furthermore, the free volume obtained from PALS experiments has been interpreted in terms of the Simha - Somcynsky theory.

Previous investigators have deduced the free volume distribution of polymer melts from molecular dynamics (MD) and Monte Carlo (MC) simulations. Takeuchi and coworkers[13] extracted a free volume distribution from the radial distribution function obtained from MD simulations on polyethylene. Tamai and coworkers[14] identified the free volume distribution with the insertion probability for inserting a spherical cavity into

polydimethyl siloxane and polyethylene liquids modeled with MD simulations. Recently Bharadwaj and Boyd[15] performed similar free volume distribution calculations based on MD simulations of a number of polymer liquids. Greenfield and Theodorou[16] used a tesselation approach to extract anisotropic free volume distributions from MC and energy minimization simulations on liquid and glassy atactic polypropylene.

Curro and Schweizer[17] developed the polymer reference interaction site model or PRISM theory for modeling the structure and thermodynamic properties of polymer melts and blends. PRISM theory is based on liquid state theoretical methods and has as its primary output information about the structure, or packing, of the polymer liquid. This structural information can be used to extract the insertion probability, or the chemical potential for inserting a spherical particle of a given diameter into the polymer. In fact this method was used previously by Curro, Honnell, and McCoy[18] to calculate the solubility of monatomic gases in polymers. In the present investigation we use PRISM theory to calculate the probability of inserting a spherical cavity into a homopolymer melt. By studying this insertion probability as a function of the cavity size, we are able to extract the free volume distribution of the polymer. We will gage the accuracy of the theoretical free volume distributions by comparing with exact results from MD simulations on a coarse grained model. Furthermore we will use PRISM theory to model the free volume distribution of polyethylene and polyisobutylene melts.

An interesting question that can be addressed, if one has a quantitative measure of the free volume distribution, concerns the relationship between free volume and physical properties. Can dynamical phenomena, such as diffusion, be correlated with the free volume distribution, an inherently static, equilibrium quantity? Although we will briefly

touch on this question, the primary purpose of this investigation is to demonstrate that the free volume distribution can be computed from integral equation theory.

THEORY AND SIMULATION

PRISM theory[17,19,20,21] is an extension to polymers of the reference interaction site model of Chandler and Andersen[22,23] of molecular liquids. Since the theory is based on liquid state physics concepts, the output is information regarding the structure of the liquid expressed through a set of intermolecular pair correlation functions $g_{\alpha\gamma}(r)$ between interaction sites α and γ on different macromolecules (see Fig. 1). The intermolecular packing $(h_{\alpha\gamma}(r) = g_{\alpha\gamma}(r) - 1)$ is related to the intramolecular structure through a generalized Ornstein-Zernike equation[17]

$$\underset{\sim}{\hat{h}}(k) = \underset{\sim}{\hat{\Omega}}(k) \cdot \underset{\sim}{\hat{C}}(k) \cdot \left[\underset{\sim}{\hat{\Omega}}(k) + \underset{\sim}{\rho} \cdot \underset{\sim}{\hat{h}}(k) \right] \tag{1}$$

where the caret denotes the Fourier transform with wave vector k and $\underset{\sim}{\rho}$ is the diagonal matrix of site densities ρ_α of type α. The average intramolecular structure of a chain of N monomers is characterized by the single-chain structure factor defined as

$$\hat{\Omega}_{\alpha\gamma}(k) = \frac{1}{N_\alpha} \sum_{i \in \alpha} \sum_{j \in \gamma} \left\langle \frac{\sin kr_{ij}}{kr_{ij}} \right\rangle \tag{2}$$

where N_α is the number of sites of type α per chain. The indices i and j in Eq. (2) sum over the sites of type α and γ on the chain.

The generalized Ornstein-Zernike equation also involves the matrix $C_{\alpha\gamma}(r)$ known as the direct correlation function. For van der Waals interactions at liquidlike densities, it

can be demonstrated[17,24] that the direct correlation function is a short range function of distance. Based on this idea $C_{\alpha\gamma}(r)$ can be approximated by the Percus-Yevik closure[17,24]

$$C_{\alpha\gamma}(r) = \left\{1 - \exp\left[\beta v_{\alpha\gamma}(r)\right]\right\} g_{\alpha\gamma}(r) \tag{3a}$$

where $v_{\alpha\gamma}(r)$ is the united atom potential between intermolecular sites. For the case of a hard core potential the PY closure reduces to

$$\begin{aligned} g_{\alpha\gamma}(r) &= 0 \quad \text{for } r < d_{\alpha\gamma} \\ C_{\alpha\gamma}(r) &= 0 \quad \text{for } r > d_{\alpha\gamma} \end{aligned} \tag{3b}$$

where $d_{\alpha\gamma}$ is the hard core distance between sites, We start with united atom potentials of the Lennard-Jones type

$$v_{\alpha\gamma}(r) = 4\varepsilon_{\alpha\gamma}\left[\left(\frac{\sigma_{\alpha\gamma}}{r}\right)^{12} - \left(\frac{\sigma_{\alpha\gamma}}{r}\right)^{6}\right] \tag{4}$$

For dense liquids it is well established[24] that the structure of the liquid is determined by the repulsive part of the potential. This motivates us to decompose the Lennard-Jones potential into a repulsive, reference part $v_r(r)$ and an attractive, or perturbative part $v_a(r)$ following Weeks, Chandler and Andersen[25] (WCA)

$$\begin{aligned} v_r(r) &= 4\varepsilon\left[\left(\frac{\sigma}{r}\right)^{12} - \left(\frac{\sigma}{r}\right)^{6} + \frac{1}{4}\right] \quad r \le 2^{1/6}\sigma \\ v_r(r) &= 0 \qquad\qquad\qquad\qquad\quad r \ge 2^{1/6}\sigma \end{aligned} \tag{5a}$$

$$v_a(r) = -\varepsilon \qquad r \le 2^{1/6}\sigma$$

$$v_a(r) = 4\varepsilon\left[\left(\frac{\sigma}{r}\right)^{12} - \left(\frac{\sigma}{r}\right)^{6}\right] \qquad r \ge 2^{1/6}\sigma \tag{5b}$$

Previous work[17] has demonstrated that PRISM theory works best for repulsive potentials. For this reason we employ the WCA repulsive branch of the LJ potential in the closure relation in Eq. (3). We can also approximate the soft repulsive potential in Eq. (5a) by an equivalent hard core potential with a hard core diameter d given by the Barker-Henderson relation[24,26]

$$d = \int_0^\infty \left\{1 - \exp\left[-\beta v_r(r)\right]\right\} dr \tag{6}$$

where as usual $\beta = 1/k_B T$. The potential parameters and equivalent hard sphere diameters used in this work are given in Table 1.

If we know the average intramolecular structure functions specified through $\hat{\Omega}_{\alpha\gamma}(k)$ in Eq. (2), then the generalized Ornstein-Zernike equation in Eq. (1), together with the closure relation in Eq. (3) can be solved numerically for the intermolecular packing correlations $g_{\alpha\gamma}(r)$. To first order, one can approximate $\hat{\Omega}_{\alpha\gamma}(k)$ through the Flory ideality hypothesis[17,27] by assuming that long range excluded volume interactions are screened in the bulk polymer liquid. Thus effectively we assume that the intramolecular structure of the polymers is ideal in the melt. Another approach is to take $\hat{\Omega}_{\alpha\gamma}(k)$ from a full, many chain MD simulation if this information is available. We will do this in the present investigation for a coarse grained polymer model. In the absence of exact many chain simulations, we can solve for both the intra and intermolecular structure in a self-consistent manner[17].

In the self-consistent approach, one performs a single chain simulation with all intramolecular repulsive interactions turned on. The effect of the surrounding chains is mimicked through a self-consistently determined solvation potential $W_{\alpha\gamma}(r)$ acting between all pairs of intramolecular sites. The form of the solvation potential was taken to be[17]

$$\beta\hat{W}_{\alpha\gamma}(k) = -\sum_{i,j}\hat{C}_{\alpha i}(k)\hat{S}_{ij}(k)\hat{C}_{j\gamma}(k) \tag{7}$$

where the partial structure factor matrix is defined according to

$$\hat{S}_{\alpha\gamma}(k) = \rho_\alpha\hat{\Omega}_{\alpha\gamma}(k) + \rho_\alpha\rho_\gamma\hat{h}_{\alpha\gamma}(k) \tag{8}$$

Self consistent calculations of this type have been carried out recently on polyethylene[28] (PE), isotactic polypropylene (iPP), syndiotactic polypropylene (sPP), polyisobutylene[29] (PIB), head-to-head polypropylene (hhPP), and poly (ethylene propylene)[30] (PEP).

Chandler and Pratt[23,31] showed that the chemical potential for inserting a hard sphere particle into a liquid could be found by growing the particle from a point. This approach was used by Pratt and Chandler[31] to calculate the Henry's law constant for methane in water. The formalism was also employed by Curro and coworkers[18] to compute the solubility of monatomic gases in polymers. Following Chandler[23] we can write the chemical potential μ, suitably modified for multisite polymers[13], for inserting a hard sphere of diameter D into a polymer melt of monomer density ρ_m as

$$\beta\mu = \beta\mu_0 + \frac{\pi D\rho_m}{2}\sum_\alpha\int_0^1 d\lambda(d_\alpha + \lambda D)^2 g^\lambda_{\alpha D}\left(\frac{d_\alpha + \lambda D}{2}\right) \tag{9}$$

with μ_0 being the chemical potential of an ideal gas of particles. The sum in the above equation extends over all sites constituting the monomer structure. Eq. (9) is written in

the Henry's law limit where the particle concentration is taken to zero. $g^{\lambda}_{\alpha D}[.5(d_\alpha + \lambda D)]$ is the contact value of the pair correlation function between a particle of diameter λD and a site on a polymer chain of type α. Eq. (9) is a charging integral that grows the particle from a point to diameter D as the charging parameter λ varies from 0 to 1. In the solubility calculations of Curro[13] et. al. PRISM theory was used to compute the contact pair correlation function as a function of the charging parameter. It should be pointed out that Eq. (9) is written for the case where both the particle being inserted and the polymer sites interact with hard core potentials. Although Eq. (9) can be generalized[23] to soft potentials, the implementation is much simpler for the hard core interactions. In the present investigation we will consider the hard core case where the hard core site diameters d_α are computed from the Lennard-Jones parameters using Eqs. (5) and (6).

We now make use of the fact that the chemical potential for inserting a spherical cavity into a liquid is the same as for a hard sphere. The only difference[23] between a cavity and a hard sphere is that cavities do not interact with each other. In the Henry's law limit, therefore, Eq. (9) also represents the chemical potential for inserting a cavity of diameter D=2R into a polymer melt. Another interpretation is that the reversible work for growing a spherical hole of radius R is $w(R) = \mu(R) - \mu_0$. Thus we can write

$$\beta w(R) = \pi R \rho \sum_{\alpha} \int_0^1 d\lambda (d_\alpha + 2\lambda R)^2 g^{\lambda}_{\alpha D}\left(\frac{d_\alpha + 2\lambda R}{2}\right) \qquad (10)$$

In this investigation we define the free volume V_f as simply the empty space existing between and among the polymer molecules, where the chains are modeled with overlapping hard sphere sites. According to this definition, the fraction f_0 of the total volume that is free is

$$f_0 = \frac{V_f}{V} = (1-\eta) \tag{11}$$

where η is the packing fraction of the polymer molecules. The question we would like to answer is how this free volume is distributed. We can use the reversible work for growing a cavity given by Eq. (10) to compute the insertion probability P(R) for finding a spherical cavity of radius R in the polymer liquid[8].

$$P(R) = f_0 \exp[-\beta w(R)] \tag{12}$$

The coefficient in Eq. (12) is required because the probability of inserting a point is given by the free volume fraction. We now identify the free volume distribution f(R) as the probability of finding a spherical cavity with a radius in the range R and R+DR. This can be related to the insertion probability through

$$f(R) = -\frac{\partial P}{\partial R}, \quad P(R) = \int_R^\infty f(R')dR' \tag{13}$$

From Eqs. (12) and (13) we see that f(R) is normalized to f_0 since the integral over all possible cavity radii must be the total free volume fraction. It is apparent that Eqs. (1) and (3) can be used to compute the contact pair correlation in Eq. (10) which can then be used to obtain the free volume distribution for a particular polymer model.

In order to assess the accuracy of using PRISM theory for obtaining the free volume distribution, we also performed MD simulations on coarse grained and atomistic polymer models. The MD simulations were run using the LAMMPS code developed by Plimpton[31] and used previously to study diffusion of penetrants in polymer melts[32]. The MD methodolgy[33] is based on a Verlet algorithm. Snapshots were periodically taken and analyzed to obtain the free volume distribution.

RESULTS AND DISCUSSION

A) Coarse-grained Model

We first applied PRISM theory to compute the free volume distribution of a coarse-grained, semiflexible chain model consisting of tangent sites depicted in Fig.1. We introduce chain stiffness into this model, as was done in an earlier study[32], through a harmonic bond angle bending potential.

$$E = K(\theta - \theta_0)^2 \tag{14}$$

where θ is the bond angle (see Fig. 1) and $\theta_0 = 120°$. As the stiffness (in units of k_BT) is varied from zero to infinity we pass from a freely jointed to a freely rotating chain. In practice a K value of 20, the maximum value in the present study, leads essentially to the freely rotating, $K \to \infty$ limit. All the coarse grained calculations were for the case of N=50 repeat units.

From MD simulations on this model we extracted the single chain structure factors as defined in Eq. (2). A Kratky plot of these single chain functions is shown in Fig. 2 for various chain stiffnesses. It can be demonstrated[17] that the plateau occurs at $k^2\hat{\omega}(k) = 12/\sigma^2$ in the intermediate scaling regime $(1/\sigma < k < 1/R_g)$. Therefore, as seen in Fig. 2, the plateau decreases as the stiffness parameter increases since the effective statistical segment length σ increases with K. These single chain structures factors were used as input to PRISM theory in Eq. (1) which, together with the closure in Eq. (3a), was solved for the intermolecular pair correlation functions g(r). Standard Picard iteration[17] was used to find numerical solutions to the integral equation. The soft, repulsive potential from Eq. (5a) was used with the Lennard-Jones parameters given in Table 1.

Fig. 3 depicts the pair correlation functions obtained from PRISM theory at three different stiffness parameters K=0, 1, 20. It can be seen from this figure that g(r) becomes larger near contact as the chain stiffness increases. This is as expected[17] because more intermolecular overlap can occur as the chains become extended. At the same time there are fewer intramolecular contacts since the average distance between intramolecular pairs increases as the chains become stiffer. This behavior was observed previously by Honnell and coworkers[34] for semiflexible chain models.

We now focus on using PRISM theory to determine the insertion probability of these semiflexible chain liquids. PRISM calculations were performed for a mixture of tangent site, hard sphere chains with site diameters (d=1.0156) and holes consisting of spherical sites of diameter $2\lambda R$ in the infinite dilution of holes limit. The intramolecular structure factor of the polymer, $\hat{\Omega}_{pp}(k)$, was taken from the MD simulations shown in Fig. 2. From Eq. (2) it can be seen that for a spherical void (or particle), $\hat{\Omega}_{vv}(k) = 1$ while the cross term can be shown to be $\hat{\Omega}_{pv}(k) = 0$. This intramolecular structure factor matrix was inserted into Eqs. (1) and (3b) to calculate the polymer/void intermolecular radial distribution function at contact as the charging parameter λ varies from 0 to 1. The contact g was then used in Eqs. (10) and (11) to obtain the reversible work for inserting a cavity. For the case of a tangent hard sphere chain the total free volume fraction f_0 is easily found to be $f_0 = 1 - \pi d^3 \rho_m / 6$. The insertion probability P(R) can now be obtained from Eq. (12). The results are shown for the flexible chain case with K=0 as the solid curve in Fig. 4.

The dotted curves in Fig. 4 were obtained from the MD simulation for the K=0 flexible chain liquid. It can be seen that there is excellent agreement between PRISM

theory and the exact simulations for small free volume void sizes. In the inset we emphasize the tail of the distribution by plotting log P(R). We can observe from the inset in Fig. 4 that the probability of inserting a cavity of volume comparable to the monomer volume is very small (~10^{-4}). We also note that PRISM theory predicts a larger insertion probability than the MD simulation for larger cavity sizes in the tail of the distribution. This is not surprising since it has been demonstrated previously[28] that PRISM theory tends to overestimate the compressibility of polymer melts. Since it is easier to insert a particle into a more compressible medium, one would expect the insertion probability to increase with compressibility.

We can approximately correct PRISM theory to give the correct compressibility by adding a tail function to the direct correlation function $C_{pp}(r)$ between polymer sites outside the hard core. This is accomplished by modifying the hard sphere closure in Eq. (3b) with a power law for the direct correlation function as was done previously[28]

$$g_{pp}(r) = 0 \quad \text{for} \quad r < d_{pp}$$

$$C_{pp}(r) = C_{HC}(d_{pp})\left(\frac{d_{pp}}{r}\right)^{\lambda} \quad \text{for} \quad r > d_{pp} \tag{3c}$$

where the exponent λ is chosen to require the isothermal compressibility κ_T to agree with experiment or simulation. We found that by taking $\lambda = 15$ we obtained numerical agreement between the zero wave vector structure factors ($\hat{S}(0) = \rho_m k_B T \kappa_T$) from PRISM theory and MD simulation of a flexible polymer melt (K=0). Eq. (3c) was then used (with λ=15) in the PRISM calculation of the polymer/void mixture to extract the insertion probability as before. It should be mentioned that the closure in Eq. (3b) was still used to describe $C_{vv}(r)$ between cavities, and the cross term $C_{pv}(r)$. This result is

shown in Fig. 4 as the dashed curve in the inset. It can be seen that some improvement in the PRISM calculation of the insertion probability is obtained in the tail of the distribution when the theory is corrected for the compressibility.

Eq. (13) can be used to obtain the free volume distribution f(R) by numerical differentiation of the insertion probability. The results for the free volume distributions of the flexible chain liquid are shown in Fig. 5 for both the theory and simulation. As for the insertion probability, reasonable agreement between theory and simulation is seen in f(R) for small free volume cavities. It will be noticed that there appears to be a maximum in the free volume distribution in the range $0 < R < 0.1$. It should be mentioned that the shape of the free volume distribution near R=0 is somewhat sensitive to the numerical uncertainties in taking the derivative of P(R). The tail of the distribution is emphasized in the inset as a plot of log f(R) versus R^2. Inspection of these curves reveals that they are nonlinear indicative of a nonGaussian character in the distribution. As we observed for the insertion probability, PRISM theory predicts the free volume distribution to be larger than the MD simulation for large cavity sizes. When we correct for compressibility we improve the agreement as can be seen in the inset of Fig. 4.

We also obtained the insertion probabilities and free volume distributions from PRISM theory and MD simulation for semiflexible chains with nonzero stiffness parameters up to K=20. Even though significant chain stiffness effects were apparent in the intramolecular structure (Fig. 2), and the intermolecular packing (Fig. 3), practically no differences were observed in P(R) and f(R) as a function of chain stiffness. We can characterize the free volume distributions through an average cavity radius $\langle R \rangle$

$$\langle R^n \rangle = \int_0^\infty R^n f(R) dR \qquad (15)$$

and the breadth of the distribution by $\langle R^2 \rangle - \langle R \rangle^2$. The values obtained from both PRISM and MD simulation are tabulated in Table 2 as a function of the chain stiffness parameter K. It can be seen from the table that both the average cavity radius and the breadth of the free volume distribution are independent of chain stiffness.

B) Realistic Models

While coarse-grained models are useful for predicting properties on long length scales such as the radius of gyration, thermodynamic properties are sensitive to local packing at the monomeric length scale. In order to see if the geometry of the monomer structure influences the free volume distribution, we studied atomistic models of polyethylene (PE) and polyisobutylene (PIB). The repeat units of these polymers are constructed from overlapping sites as shown schematically in Fig. 1. In the case of PE each site represents a CH_2 unit. For PIB we have three independent sites denoted as A, B, and C corresponding respectively to CH_2, C, and CH_3 groups. Bond lengths were maintained constant at 1.54 A; bond angle and torsional angle potentials, as well as, nonbonded potentials, were taken from Jorgensen et. al.[35] for PE, and Martin and Siepmann[36] for PIB.

Self consistent PRISM theory has been applied previously to these models of polyethylene[28] and polyisobutylene[29,30] liquids. The intermolecular pair correlation functions for both PE (N=66 monomers) and PIB (N=12 monomers) liquids are given in Fig. 6. Note in the case of PIB, six independent radial distribution functions $g_{\alpha\gamma}(r)$ are required to completely characterize the intermolecular packing. As expected, $g_{CC}(r)$ is

large near contact since the C groups (CH_3) are on the outside of the chain and can approach each other unhindered in the melt. At the same time correlations between backbone sites are shielded by the pendant methyl groups and this is reflected in $g_{AA}(r)$ and $g_{BB}(r)$ approaching zero well before contact.

The intramolecular structure functions $\hat{\Omega}_{\alpha\gamma}(k)$ from these earlier studies[28,30] were used in the present investigation as input to PRISM theory of the polymer/void mixture. In this manner we calculated the contact $g^{\lambda}_{\alpha D}$ appearing in Eq. (10) as a function of the charging parameter λ. The reversible work for growing a spherical cavity of radius R was then found by numerically integrating Eq. (10).

In the case of the tangent site model we were able to calculate the packing fraction of polymer in the liquid. For the overlapping site models we are now considering, analytical determination of the packing fraction is very difficult due to the existence of not only binary overlaps, but also three and four body overlaps of the sites. For this reason we estimated the packing fractions of PE and PIB, given in Table 2, from MD simulations of the probability for inserting a point into the liquid. Since MD simulations were not performed for PE at 298K, we estimated the packing fraction at this temperature from its value at 448K from the approximate relation

$$\eta(T) \cong \left(\frac{\eta}{d^3 \rho_m} \right)_{448} d^3 \rho_m \qquad (16)$$

where the effective hard core diameters and monomer densities are given Table 2. From Table 2 we see that the total free volume fraction f_0 of PIB at $(f_0 = 0.407, 0.482)$ at 298K and 453K is smaller than for PE $(f_0 = 0.426, 0.519)$ at 298K and 448K. This is consistent

with the notion that PIB macromolecules pack more efficiently in the melt than other polymers at the same temperature.

Eqs. (12) and (13) can now be employed to compute the insertion probability and free volume distribution of PE and PIB. A comparison of these two polymers is given in Fig. 7 at elevated temperature and Fig. 8 at room temperature From these figures it can be seen that the free volume distributions of PE and PIB are remarkably similar considering the differences in monomer architecture. Nonetheless we see that PIB has more of its free volume distributed in smaller size voids than is the case for PE. Qualitatively similar behavior was observed by Bharadwaj and Boyd[15] for the insertion probabilities of PE and PIB. The total free volumes, or the insertion probability for inserting a point P(0), reported by Bharadwaj and Boyd are larger than ours because they defined the hard core diameter of a site as the Lennard-Jones σ parameter, whereas we use the WCA definition of d obtainable from Eqs. (5) and (6).

C) Penetrant Diffusion

It would be highly desirable if dynamical properties of a polymer could be correlated with its static or equilibrium structure in the bulk liquid. An example of such a correlation was made many years ago by Cohen and Turnbull[6] who argued that the diffusion constant D_p of a penetrant, such as a gas molecule diffusing through a liquid, would be proportional to the free volume larger than the penetrant size. Thus Cohen and Turnbull suggest that the diffusion constant of a molecule of radius R* is proportional to the insertion probability.

$$D_p \propto \int_{R^*}^{\infty} f(R)dR = P(R^*) \qquad (17)$$

Since we find that for semiflexible chains the free volume distribution is essentially independent of chain stiffness, Eq. (17) would suggest that the penetrant diffusion constant would also be independent of the stiffness parameter K.

In order to test this hypothesis, we studied[32] the diffusion of monomeric penetrants in the same semiflexible chain melts discussed earlier. The diffusion constants of spherical penetrants, having their radius the same as the polymer repeat unit, were obtained from MD simulations[†] as in an earlier study[32]. D_p was extracted from particle trajectories making use of the Einstein relation.

$$D_p = \lim_{t\to\infty}\left\langle \frac{r^2}{6t} \right\rangle \tag{18}$$

The results are shown in Table 3. Surprisingly, we find that the penetrant diffusion constant is not independent of chain stiffness as Eq.(17) would suggest, but decreases by about a factor of two as the chains pass from freely jointed to freely rotating. Apparently that in addition to the free volume distribution, other factors also are important in controlling the diffusion constant. It should be mentioned, however, that extraction of diffusion constants from MD simulations is subject to uncertainties because of difficulties in getting into the diffusive, or Fickian regime.

It is well known that PIB, the polymeric component of butyl rubber, exhibits an extraordinarily low diffusion constant for gases compared to other similar polyolefins. For example, the diffusion constant of N_2 through butyl rubber is approximately seventeen times smaller[37] than for ethylene propylene at room temperature. The effective hard core diameter for N_2 using Eqs. (5) and (6) is 3.58 A. From the data shown in Fig. 8, we can estimate the ratio of the insertion probabilities of PE to PIB is approximately nine

for inserting a particle of diameter 3.58 A. Thus we find qualitative agreement with the relationship between diffusion constant and free volume distribution given in Eq. 17.

CONCLUSIONS

In this investigation we have defined the free volume distribution in terms of the insertion probability for inserting a spherical cavity into the polymer liquid. With this definition we can compute the free volume distribution from both PRISM theory and MD simulations. Comparisons between theory and simulation demonstrates that PRISM theory is capable of accurately predicting the free volume distribution at small cavity sizes. However, in the tail of the free volume distribution, PRISM theory, because the compressibility is too high, tends to overestimate the insertion probability for inserting larger cavities.

In the case of semiflexible chain liquids, we find from both MD simulation and PRISM theory that the free volume distribution is essentially independent of chain stiffness. The diffusion constant of monomer sized penetrants does seem to decrease as the polymer changes from a freely joined to a freely rotating chain. These observations tentatively lead us to the conclusion that Cohen and Turnbull's conjecture, that diffusion is related to the free volume distribution through Eq. (17), is not rigorously correct based on our definition of free volume. We do find qualitative agreement with Cohen and Turnbull in the case of the relative diffusion constants of N_2 in PIB and PE.

Further study is necessary in order to determine whether our calculational method for estimating the free volume distribution in polymer liquids could be useful in predicting, at least in a relative sense, other nonequilibrium properties such as glass transitions.

REFERENCES

† In reference 32 there was an error in the MD simulations for semiflexible chains with stiffnesses in the range K=0 to 10. These runs were repeated with results given in Table 3.

1. Ferry, J. D, *Viscoelastic Properties of Polymers*, John Wiley & Sons, New York, (1980).

2, Kovacs, A., *Adv. Polym. Sci.*, **1964**, 3, 394.

3. Curro, J. G.; Lagasse, R. R.; Simha, R.; *J. Appl. Phys.*, **1981**, 52, 5892; *Macromolecules*, **1982**, 15, 1621.

4. Robertson, R. E.; Simha, R.; Curro, J. G.; *Macromolecules*, **1984**, 17, 911.

5. Doolittle, A. K., *J. Appl. Phys.*, **1951**, 22, 1471.

6. Cohen, M. H.; Turnbull, D.; *J. Chem. Phys.*, **1959**, 31, 1164.

7. Pant, P. V. K., Boyd, R.; *Macromolecules*, **1992**, 25, 494..

8. Reiss, H.; Hammerich, A. D.; *J. Phys. Chem.*, **1986**, 90, 6252.

9. Simha, R.; Somcynsky, T.; *Macromolecules*, **1969**, 2, 342.

10. Kobayashi, Y.; Zheng, W.; Meyer, E. F.; McGervey, J. D.; Jamieson, A. M.; Simha, R.; *Macromolecules*, **1989**, 22, 2302.

11. Yu, Z.; Yashi, U.; McGervey, J. D.; Jamieson, A. M.; Simha, R.; *J. Polym. Sci. B*, **1994**, 32, 2637.

12. Kobayashi, Y.; Haraya, K.; Hattori, S.; Sasuga, T.; *Polymer*, 35, 925.

13. Takeuchi, H.; Roe, R. J.; Mark, J. E., *J. Chem. Phys.*, **1990**, 93, 9042.

14. Tamai, Y.; Tanaka, H.; Nakanishi, K.; *Macromolecules*, **1994**, 27, 4498.

15. Bharadwaj, R. K.; Boyd, R. H.; *Polymer*, **1999**, 40, 4229.

16. Greenfield, M. L.; Theodorou, D. N.; *Macromolecules*, **1993**, 26, 5461.

17. For recent reviews see: Schweizer, K. S.; Curro, J. G.; *Adv. Polym. Sci.*, **1994**, 116, 321. Schweizer, K. S.; Curro, J. G.; *Adv. Chem. Phys.* **1997**, 98, 1.

18. Curro, J. G.; Honnell, K. G.; McCoy, J. D.; *Macromolecules*, **1997**, 30, 145.

19. Schweizer, K. S. and Curro J. G. *Phys. Rev. Lett.* **1987**, **58**, 246.

20. Curro, J. G. and Schweizer, K. S. *Macromolecules* **1987**, 20, 1928.

21. Curro, J. G. and Schweizer, K. S. *J. Chem. Phys.* **1987**, 87, 1842.

22. Chandler, D.; Andersen, H. C. *J. Chem. Phys.* **1972**, 57, 1930.

23. Chandler, D. in *Studies in Statistical Mechanics VIII*, edited by Montroll, E. W.; Lebowitz, J. L., North-Holland, Amsterdam, 1982.

24. Hansen, J. P.; McDonald, I. R. *Theory of Simple Liquids*, 2nd ed., Academic: New York, 1986.

25. Weeks, J. D., Chandler, D., and Andersen, H. C., *J. Chem. Phys.*, **1971**, 54, 5237.

26. Barker, J. A.; Henderson, D.; *J. Chem. Phys.*, **1967**, 47, 4714.

27. Flory, P. J., *J. Chem. Phys.*, **1949**, 17, 203.

28. Curro, J. G.; Webb, E. B.; Grest, G. S.; Weinhold, J. D.; Pütz, M.; McCoy, J. D.; *J. Chem. Phys.*, **1999**, 111, 9073.

29. Weinhold, J. D.; Curro, J. G.; Habenschuss, A.; Londono, J. D.; *Macromolecules*, **1999**, 32, 7276.

30. Pütz, M.; Curro, J. G.; Grest, G. S.; *J. Chem. Phys.*, in press.

31. Plimpton, S. J.; *J. Comp. Phys.*, **1995**, 117, 1.

32. Rottach, D. R.; Tillman, P. A.; McCoy, J. D.; Plimpton, S. J.; Curro, J. G.; *J. Chem. Phys.*, **1999**, 111, 9822.

33. Allen, M. P.; Tildesley, D. J.; *Computer Simulation of Liquids*, Academic: New York, 1986.

34. Honnell, K. G.; Curro, J. G.; Schweizer, K. S.; *Macromolecules*, **1990**, 23, 3496.

35. Jorgensen, W. L.; Madura, J. D.; Swenson, C. J.; *J. Am. Chem. Soc.*, **1984**, 106, 6638.

36. Martin, M.; Siepmann, I.; *J. Phys. Chem. B*, **1999**, 103, 4508.

37. Brandrup, J.; Immergut, E. H.; Grulke, E. A.; *Polymer Handbook*, 4th Ed., John Wiley & Sons, Inc., New York **1999**.

Table 1 – Lennard-Jones Interaction Parameters

Polymer	Site	T(K)	$\varepsilon/k_B T$	σ_{LJ} (A)	d (A)
Semiflexible	bead		1.00	1.00	1.0156
PE	CH_2	448	0.1038	3.93	3.59
	CH_2	298	0.1560	3.93	3.67
PIB	CH_2	453	0.1007	3.95	3.60
	C		0.0011	6.40	4.25
	CH_3		0.2146	3.73	3.54
	CH_2	298	0.1530	3.95	3.69
	C		0.0017	6.40	4.39
	CH_3		0.3262	3.73	3.61

Table 2 – Average Free Volume

Polymer	T (K)	ρ*	η**	$\langle R \rangle^{\dagger}$	$\langle R^2 \rangle - \langle R \rangle^{2\,\dagger}$
Semiflexible					
K=0		0.8476	0.45	0.123	0.00768
				(0.119)	(0.00714)
K=1		0.8476	0.45	0.125	0.00827
				(0.119)	(0.00706)
K=5		0.8476	0.45	0.1258	0.00818
				(0.119)	(0.00704)
K=20		0.8476	0.45	0.1263	0.00823
				(0.120)	(0.00717)
PE	448	0.03294	0.481	0.452	0.113
	298	0.3678	~0.574	0.379	0.0804
PIB	453	0.00892	0.518	0.447	0.113
	298	0.00980	0.593	0.358	0.0742

*ρ is the monomer density in units of A^{-3} for PE and PIB and in units of d^{-3} for the semiflexible chains.
**The packing fraction η was estimated from MD simulations for PE and PIB
† In units of A for PE and PIB and units of d for the semiflexible chains. Values in parentheses are from MD simulations, otherwise they are from PRISM.

Table 3 – Penetrant Diffusion Constants for Semiflexible Chain Liquids

Stiffness K	D_p
0	0.045
2	0.048
10	0.023
20	0.020

FIGURE CAPTIONS

1. Schematic diagrams of the polymer chains studied. Top: a tangent site, semiflexible chain; Middle: polyethylene chain with overlapping CH_2 sites; Bottom: polyisobutylene chain with three independent sites A (CH_2), B (C), and C (CH_3).
2. Kratky plot of the single chain structure factor of semiflexible chains obtained from MD simulations with various chain stiffness. Starting from top to bottom: K=0, 1, 5, 10, 20.
3. Intermolecular radial distribution function for semiflexible chains. Top: K=20, Middle: K=1, Bottom, K=0.
4. Insertion probability P(R) for a semiflexible chain liquid with chain stiffness K=0. The solid curve is from PRISM theory, the dotted curve is from MD simulation. The inset is a plot of log P(R) versus R. The dashed curve in the inset is from PRISM theory with the compressibility correction.
5. Free volume distribution f(R) for a semiflexible chain liquid with chain stiffness K=0. The solid curve is from PRISM theory, the dotted curve is from MD simulation. The dashed curve is from PRISM theory with the compressibility correction. The inset is a plot of log f(R) versus R^2.
6. Intermolecular distribution functions for polyethylene (top) and polyisobutylene (bottom 6). The curves have been shifted along the y-axis for clarity.
7. Free volume distribution at T=298K for polyethylene (dotted curve) and polyisobutylene (solid curve) obtained from PRISM theory. The inset is the corresponding logarithmic plot of the insertion probability versus R.

8. Free volume distribution for polyethylene at 448K (dotted curve) and polyisobutylene at 453K (solid curve) obtained from PRISM theory. The inset is the corresponding logarithmic plot of the insertion probability versus R.

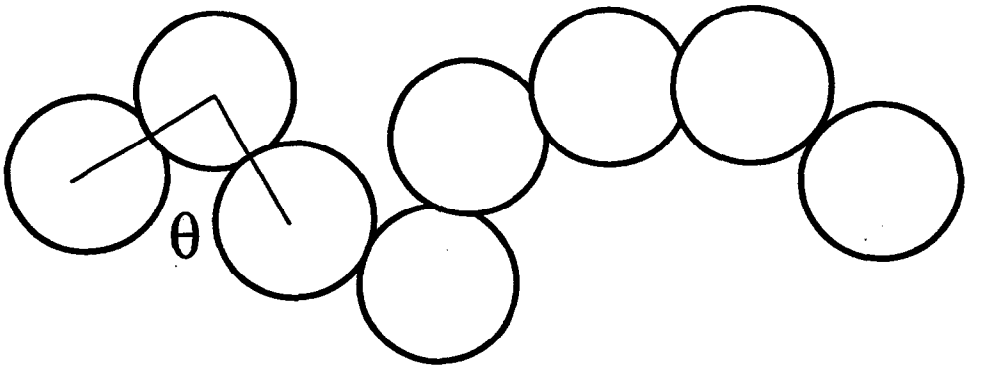
θ

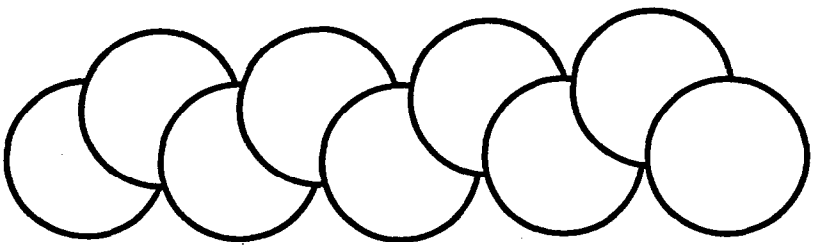

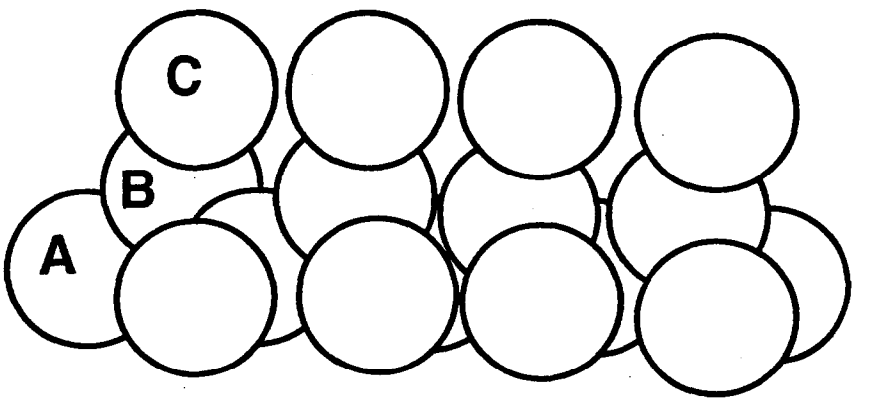
C
B
A

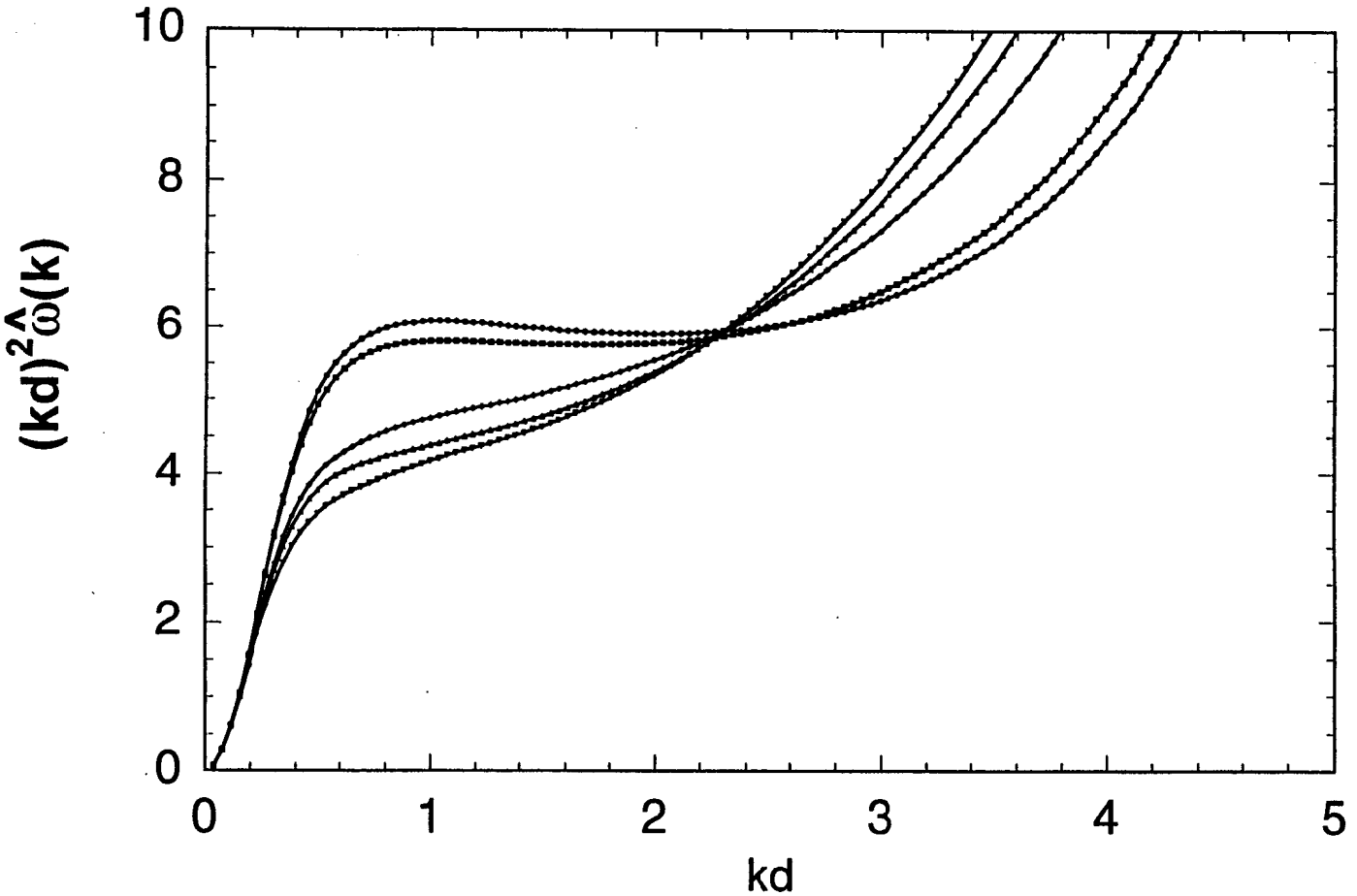
10
8
6
4
2
0
0
1
2
3
4
5
kd
(kd)^2 ω̂(k)

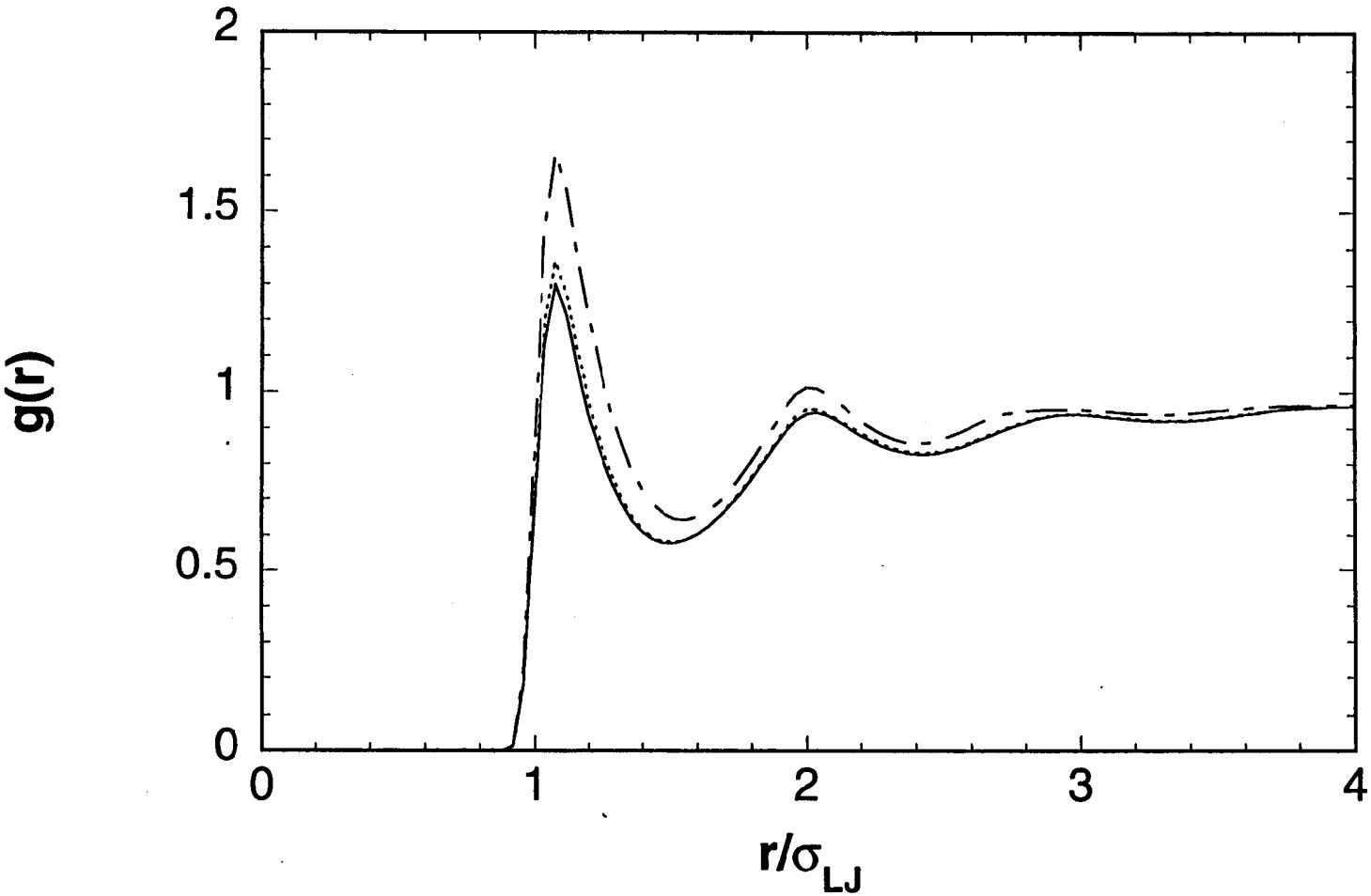
g(r)
2
1.5
1
0.5
0
0
1
2
3
4
r/σLJ

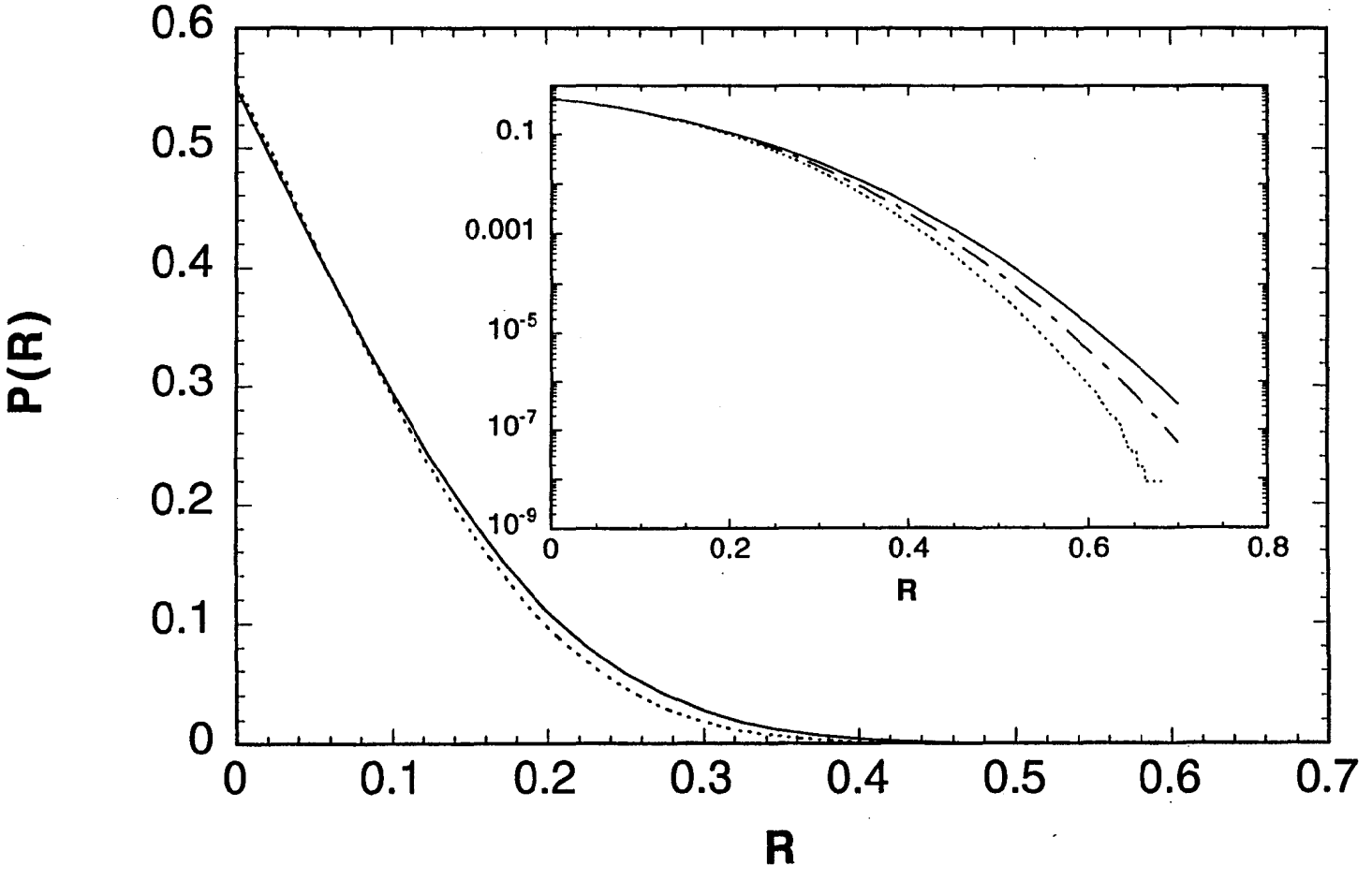
P(R)
R
0.6
0.5
0.4
0.3
0.2
0.1
0
0
0.1
0.2
0.3
0.4
0.5
0.6
0.7
0.1
0.001
10-5
10-7
10-9
0
0.2
0.4
0.6
0.8
R

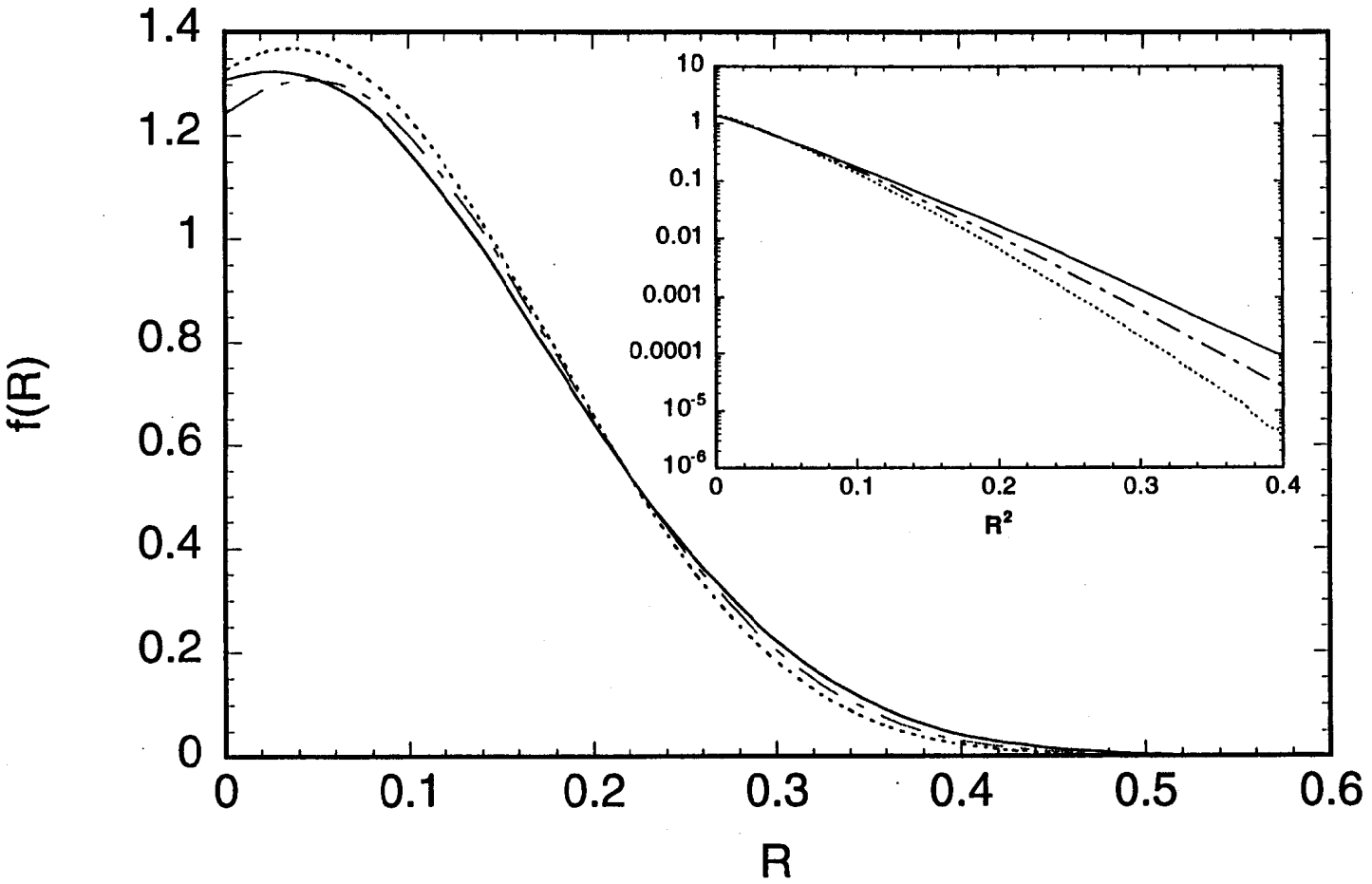
f(R)
R
1.4
1.2
1
0.8
0.6
0.4
0.2
0
0
0.1
0.2
0.3
0.4
0.5
0.6
10
1
0.1
0.01
0.001
0.0001
10-5
10-6
0
0.1
0.2
0.3
0.4
R2

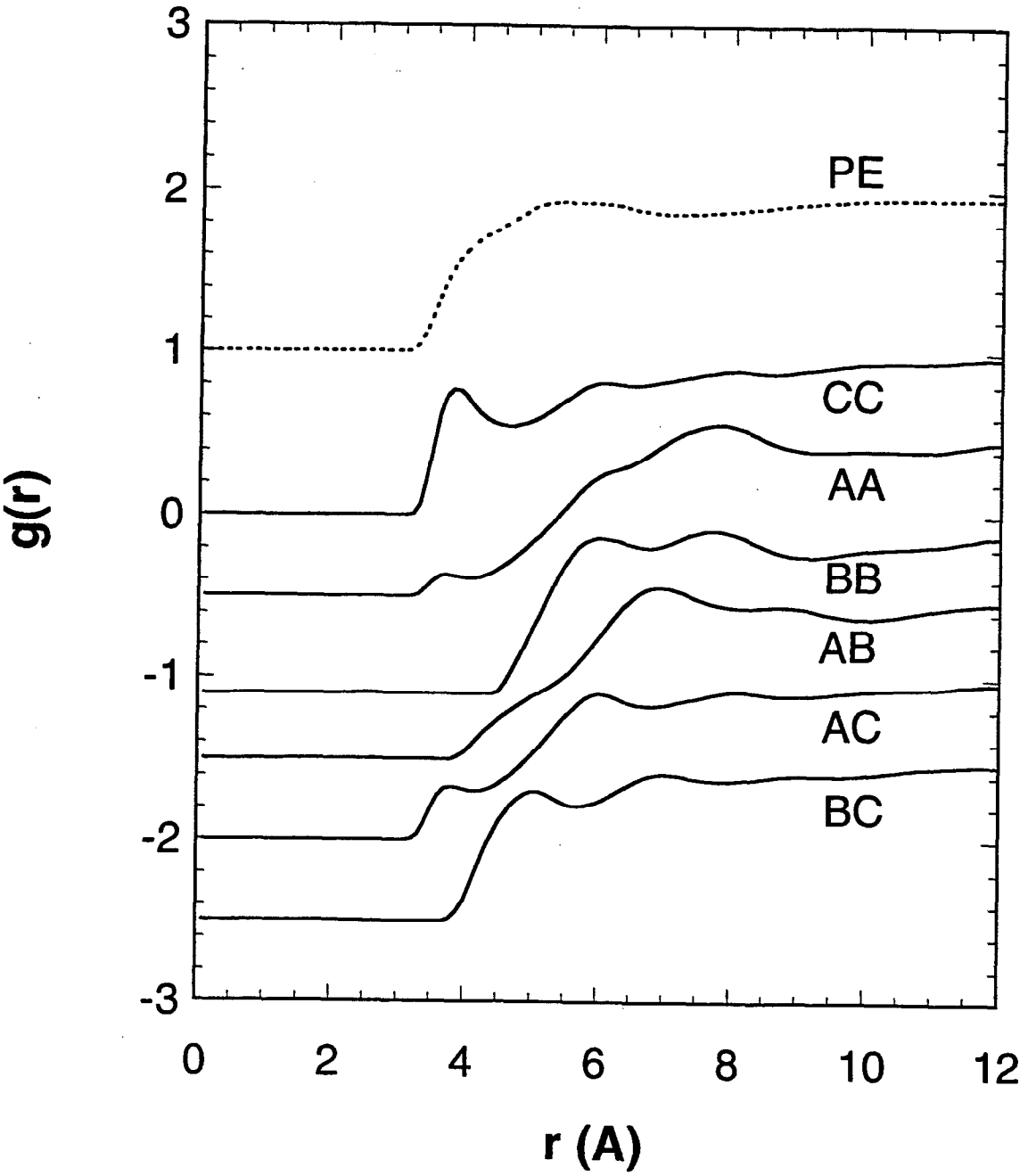
3
2
1
0
-1
-2
-3
g(r)
PE
CC
AA
BB
AB
AC
BC
0
2
4
6
8
10
12
r (A)

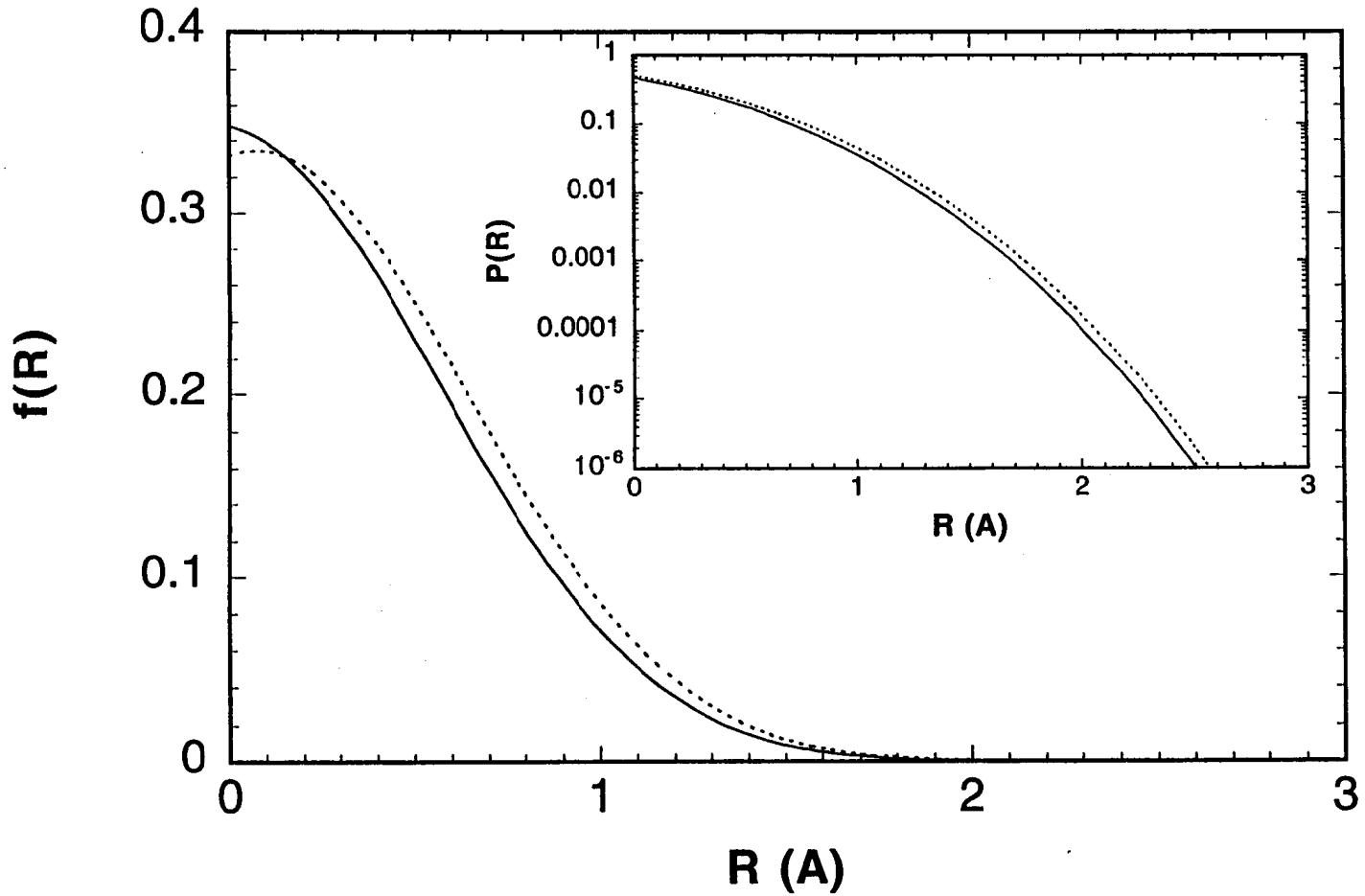
0.4
0.3
0.2
0.1
0
f(R)
0
1
2
3
R (A)
1
0.1
0.01
0.001
0.0001
10^{-5}
10^{-6}
P(R)
0
1
2
3
R (A)

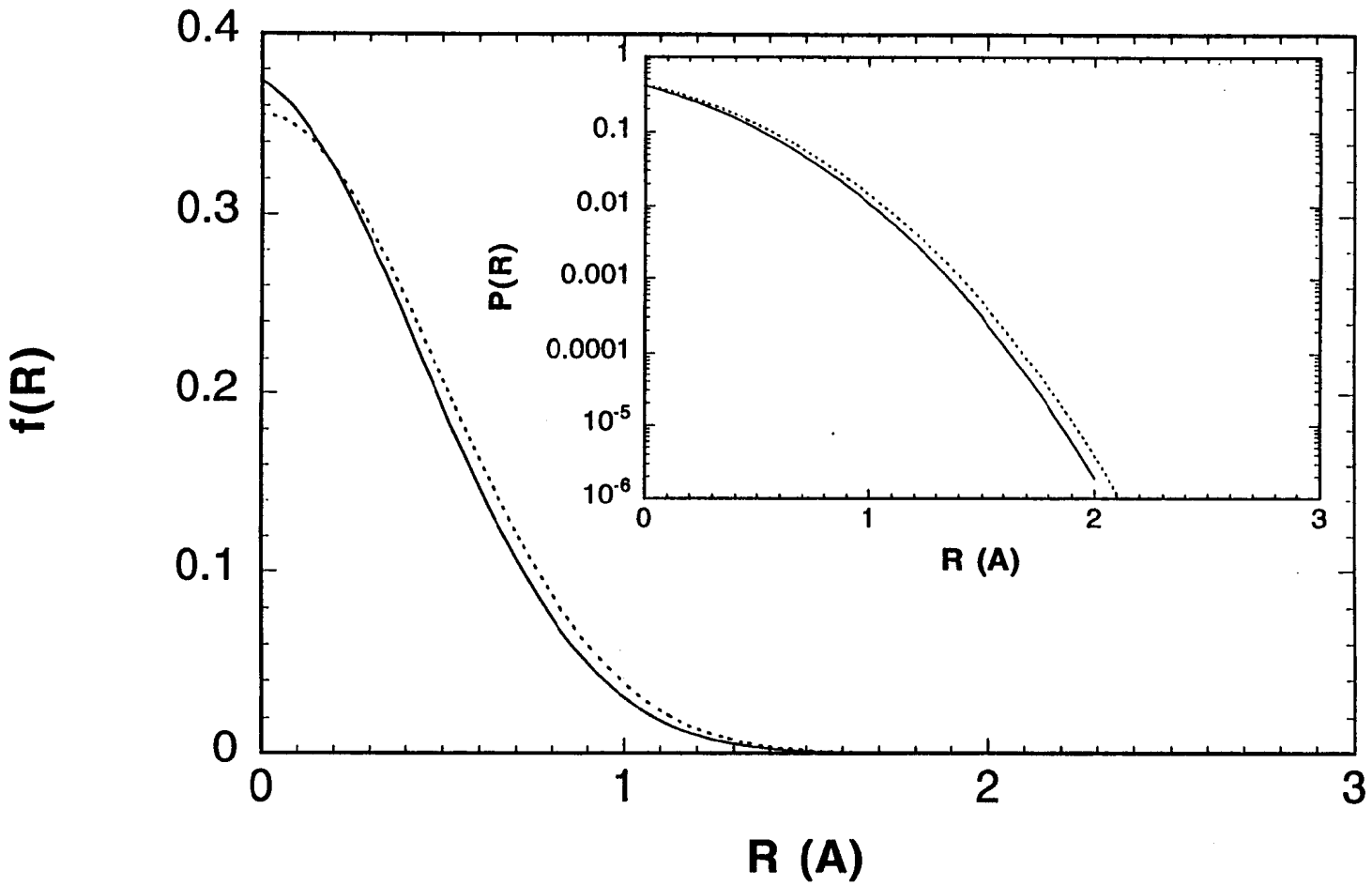
f(R)
0.4
0.3
0.2
0.1
0
0
1
2
3
R (A)
P(R)
1
0.1
0.01
0.001
0.0001
10-5
10-6
0
1
2
3
R (A)

Distribution

1	MS 0188	LDRD Office, 4001
1	1411	Gary S. Grest, 1834
1	1349	Amalie Frischknecht, 1834
1	1411	Scott Sides, 1834
10	1349	John G. Curro, 1834
1	1349	Frank van Swol, 1841
1	9018	Central Technical Files, 8945-1
2	0899	Technical Library, 9616
1	0612	Review & Approval Desk, 9612 For DOE/OSTI